



Volatile organic compounds (VOCs) from diffuse degassing areas: Interstitial soil gases as message bearers from deep hydrothermal reservoirs

Stefania Venturi^{a,b,*}, Antonio Randazzo^{a,b}, Jacopo Cabassi^b, Daniele Cinti^c, Federica Meloni^{a,b}, Monia Procesi^c, Barbara Nisi^b, Nunzia Voltattorni^c, Francesco Capecciacci^{a,b,d}, Tullio Ricci^c, Orlando Vaselli^{a,b,e}, Franco Tassi^{a,b}

^a Department of Earth Sciences, University of Florence, Via G. La Pira 4, 50121 Firenze, Italy

^b Institute of Geosciences and Earth Resources (IGG), National Research Council of Italy (CNR), Via G. La Pira 4, 50121 Firenze, Italy

^c Istituto Nazionale di Geofisica e Vulcanologia (INGV), Sezione Roma 1, via di Vigna Murata 605, 00143 Roma 1, Italy

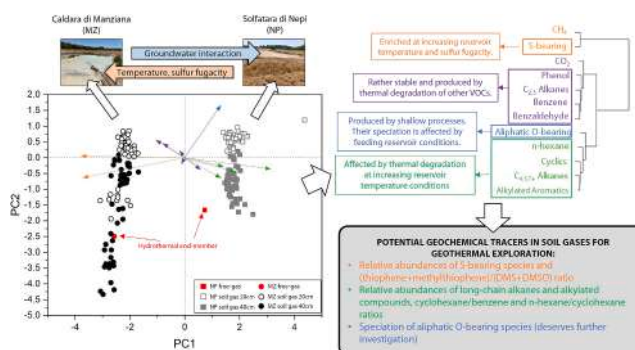
^d Istituto Nazionale di Geofisica e Vulcanologia (INGV), Sezione di Napoli, via Diocleziano 328, 80122 Napoli, Italy

^e Istituto Nazionale di Geofisica e Vulcanologia (INGV), Sezione di Bologna, viale Bertini Pichat 6/2, 40127 Bologna, Italy

HIGHLIGHTS

- Soil gases and free-gas discharges were collected from two hydrothermal areas.
- Volatile organic compounds (VOCs) showed distinct compositions in the two areas.
- VOCs speciation in soil gases roughly reflects that observed in free-gases.
- VOCs speciation is controlled by the physicochemical features of deep reservoirs.
- VOCs speciation in soil gases is a valuable tool for geothermal exploration.

GRAPHICAL ABSTRACT



ARTICLE INFO

Editor: Christian Herrera

Keywords:

VOCs
Hydrothermal reservoirs
Soil gases
Geochemical tracers
Central Italy

ABSTRACT

The chemical composition of volatile organic compounds (VOCs) in interstitial soil gases from hydrothermal areas is commonly shaped by both deep hydrothermal conditions (e.g., temperature, redox, sulfur fugacity) and shallow secondary processes occurring near the soil-atmosphere interface. Caldara di Manziana and Solfatara di Nepi, i.e., two hydrothermal systems characterized by diverse physicochemical conditions located in the Sabatini Volcanic District and Vicano-Cimino Volcanic District, respectively (Central Italy), were investigated to evaluate the capability of VOCs in soil gases to preserve information from the respective feeding deep fluid reservoirs. Hierarchical cluster analyses and robust principal component analyses allowed recognition of distinct groups of chemical parameters of soil gases collected from the two study areas. The compositional dissimilarities from the free-gas discharges were indeed reflected by the chemical features of soil gases collected from each site, despite the occurrence of shallow processes, e.g., air mixing and microbial degradation processes, affecting VOCs. Four distinct groups of VOCs were recognized suggesting similar sources and/or geochemical behaviors, as follows: (i) S-bearing compounds, whose abundance (in particular that of thiophenes) was strictly dependent on the sulfur

* Corresponding author at: Department of Earth Sciences, University of Florence, Via G. La Pira 4, 50121 Firenze, Italy.

E-mail address: stefania.venturi@unifi.it (S. Venturi).

<https://doi.org/10.1016/j.scitotenv.2023.169047>

Received 21 August 2023; Received in revised form 27 November 2023; Accepted 30 November 2023

Available online 5 December 2023

0048-9697/© 2023 The Authors. Published by Elsevier B.V. This is an open access article under the CC BY-NC-ND license (<http://creativecommons.org/licenses/by-nc-nd/4.0/>).

fugacity in the feeding system; (ii) C_{4,5,7+} alkanes, n-hexane, cyclics and alkylated aromatics, related to relatively low-temperature conditions at the gas source; (iii) C_{2,3} alkanes, benzene, benzaldehyde and phenol, i.e., stable compounds and thermal degradation products; and (iv) aliphatic O-bearing compounds, largely influenced by shallow processes within the soil. However, they maintain a chemical speciation that preserves a signature derived from the supplying deep-fluids, with aldehydes and ketones becoming more enriched after intense interaction of the hypogenic fluids with shallow aquifers. Accordingly, the empirical results of this study suggest that the chemical composition of VOCs in soil gases from hydrothermal areas provides insights into both deep source conditions and fluid circulation dynamics, identifying VOCs as promising geochemical tracers for geothermal exploration.

1. Introduction

Volatile organic compounds (VOCs) ubiquitously occur in hydrothermal gases emitted from both free-gas discharges and diffuse soil degassing areas, their origin being mainly ascribed to the presence of organic matter embedded in the geological materials (e.g., Capaccioni and Mangani, 2001; Capaccioni et al., 2001; Taran and Giggenbach, 2003; Schwandner et al., 2004; Tassi et al., 2005a, 2005b, 2010; Schwandner et al., 2013; Tassi et al., 2015a, 2015b). The physicochemical features of hydrothermal reservoirs (e.g., T, redox, sulfur fugacity) shape the speciation of organic gaseous compounds (e.g., Capaccioni et al., 1993, 1995; Venturi, 2017; Venturi et al., 2017 and references therein). Once at shallow depth, deep-sourced VOCs in up-rising hydrothermal fluids may undergo transformations, encountering sharply different physicochemical conditions and microbial communities able to exploit VOCs as carbon substrates (e.g., Hanson and Hanson, 1996; Rojo, 2009; Abbasian et al., 2015; Tassi et al., 2015a, 2015b; Venturi, 2017; Randazzo et al., 2020, 2023). Hence, in areas affected by hydrothermal fluid emissions, the composition of the released VOCs can be regarded as a chemical cocktail resulting from the co-occurrence of multiple physical, chemical and biological processes acting from the deep hydrothermal reservoirs up to the soil-atmosphere interface.

Recent studies showed that secondary processes are able to affect the composition of the organic fraction during gas migration through the shallowest 50 cm of soil from hydrothermal areas (e.g., Tassi et al., 2015a, 2015b; Venturi, 2017). The impact of shallow physicochemical and biological processes on VOCs has successfully been highlighted by comparing the chemical and isotopic features of fumarolic fluids and interstitial soil gases collected from the same hydrothermal area. Nevertheless, to the best of our knowledge, the potentiality of interstitial soil gases to preserve information on the geochemical features of deep-sourced fluids, providing an investigatory tool for geothermal exploration, has received scarce attention, leaving the use of gas discharges as more well-known and traditional choices.

The Sabatini and Vicano-Cimino Volcanic Districts (SVD and VCVD, respectively; Latium, Central Italy) offers an ideal large-scale natural laboratory to investigate the response of VOC speciation in both free-gas discharges, as representatives of deep hydrothermal fluids, and interstitial soil gases (hereafter soil gases) to variable conditions controlling the feeding hydrothermal reservoir. In both volcanic districts, a regional hydrothermal system supplies the fluid discharges occurring from the Apennines to the east to the coastline to the west. Nevertheless, a geochemical gradient in the composition of both thermal waters and gas emissions was evidenced by Cinti et al. (2014, 2017) moving from the eastern to the western sectors.

In this study, we present the results of an extensive sampling campaign of free-gas discharges and soil gases from Caldara di Manziana (hereafter MZ) and Solfatara di Nepi (hereafter NP), located in the western SVD and eastern VCVD sectors, respectively. The study is aimed at investigating the VOC speciation in fluids released from MZ and NP to highlight similarities and differences between the two areas, exploring the capability of soil gases to mimic the compositional features of the feeding hydrothermal system and provide suitable geochemical tracers

for geothermal exploration.

2. Study area

The SVD and VCVD, located in the western and eastern sectors of the peri-Tyrrhenian area of Central Italy and bordered by the Apennine chain to the east and the Tyrrhenian Sea to the west (Fig. 1a), are characterized by numerous thermal CO₂-rich gas emissions and thermal waters (Minissale, 2004). The area experienced intense extensional tectonics during the Neogene leading to horst-graben structures, crustal thinning, high heat flow and subduction-related magmatism (Cinti et al., 2014, 2017 and references therein). A regional hydrothermal reservoir is hosted in fractured Mesozoic carbonate-evaporite formations, confined by low-permeable deposits (i.e., allochthonous Ligurian flyschoid sediments and Miocene-Quaternary clay and sand-clay formations), while shallower unconfined aquifers are hosted in the volcanic rocks overlying the sedimentary rock sequence (Cinti et al., 2011; Ranaldi et al., 2016; Cinti et al., 2014, 2017 and references therein). Fluid discharges associated with the regional hydrothermal system occur in the whole SVD and VCVD, from the Apennines to the coastline, their spatial distribution being mainly governed by tectonic lineaments allowing the uprising of deep Na—Cl geothermal brines and CO₂-rich gases. The latter are mainly produced by thermometamorphic reactions within the Mesozoic limestones (Cinti et al., 2011). An E-W oriented geochemical gradient of both thermal waters and gas emissions points out a westward increasing contribution of deep-originated fluids, whereas eastward, the uprising hydrothermal fluids are more efficiently cooled and diluted by the meteoric water recharge from the nearby Apennines (Cinti et al., 2017). For the present study, two areas affected by intense hydrothermal activity were selected to represent the compositional variability of fluids from the western to the eastern sectors of the peri-Tyrrhenian area of Central Italy, i.e., MZ and NP, respectively.

MZ (Fig. 1a,b) is sited within SVD in the western sector of the peri-Tyrrhenian area, approximately 10 km W of Bracciano Lake. It is a depressed area of about 0.15 km², characterized by the absence of vegetation and the occurrence of hydrothermally-altered whitish deposits with intense diffuse degassing (Costa et al., 2008; Ranaldi et al., 2016). A small water pond with vigorous gas bubbling is present at the center of the depression emitting >13 Mg CO₂/day (Rogie et al., 2000).

NP (Fig. 1a,c) is located within VCVD in the eastern sector of the peri-Tyrrhenian area, approximately 22 km NE of MZ and about 10 km NNE of Bracciano Lake. Similarly to MZ, it is slightly depressed with respect to the surroundings. The anomalous diffuse degassing consists of hydrothermalized spots of altered whitish soils, with no vegetation cover, mainly occurring along a NE-SW lineament over a 2 km elongated area.

3. Materials and methods

3.1. Sampling and analytical methods

In each study area, 50 sites were selected for soil flux measurements and soil gas sampling (Fig. 1b,c), encompassing hydrothermally-altered

terrains and vegetated soils. Soil flux of CO₂ and CH₄ were measured at each site. The former (ΦCO₂) was determined according to the “static non-stationary accumulation chamber” (AC) method using a West Systems Co. Ltd. portable flux meter equipped with an infra-red (IR) spectrophotometer (Licor® Li-820), as detailed elsewhere (Venturi et al., 2019b). Soil CH₄ flux (ΦCH₄) determination was carried out using the “static-closed accumulation chamber” (SCC) method, according to the procedure described by Tassi et al. (2015b), with sampling time intervals of 5 min. The detection limits for ΦCO₂ and ΦCH₄ were 0.08 and 0.0003 g m⁻² d⁻¹, respectively.

Soil gases from MZ and NP (Fig. 1b,c) were collected by using a 70 cm long stainless steel probe inserted into the soil down to the chosen sampling depth (20 and 40 cm depth, except for 4 sampling sites, i.e., #1, #31, #46, #47 at MZ and 1, i.e., #18, at NP, where the soil hardness only allowed the probe to reach 20 cm depth) and connected through a

three-way valve and silicon tubing to a syringe and 12 mL glass vials (Labco Exetainer®) for sample collection (Tassi et al., 2015a). At each site, soil gases were first collected at 20 cm depth and then the probe was inserted deeper in the soil down to 40 cm depth in order to grab the deeper soil gas sample. The choice of the two sampling depths (20 and 40 cm) was aimed at identifying variations in the chemical features of VOC related to very shallow secondary processes occurring within the soil able to modify the original composition of the deep-sourced fluids. As representatives of deep fluids, free gases from the bubbling pool at the center of the study area (MZ FG) and a small dry vent (NP FG) were collected at MZ and NP, respectively (Fig. 1b,c), in pre-evacuated glass flasks containing 20 mL of 4 M NaOH (Tassi et al., 2015b) connected with a silicone tube to (i) a funnel upside-down positioned above the emission and (ii) a 70 cm long stainless steel probe, respectively. Moreover, a further aliquot was transferred to 12 mL glass vials for VOCs

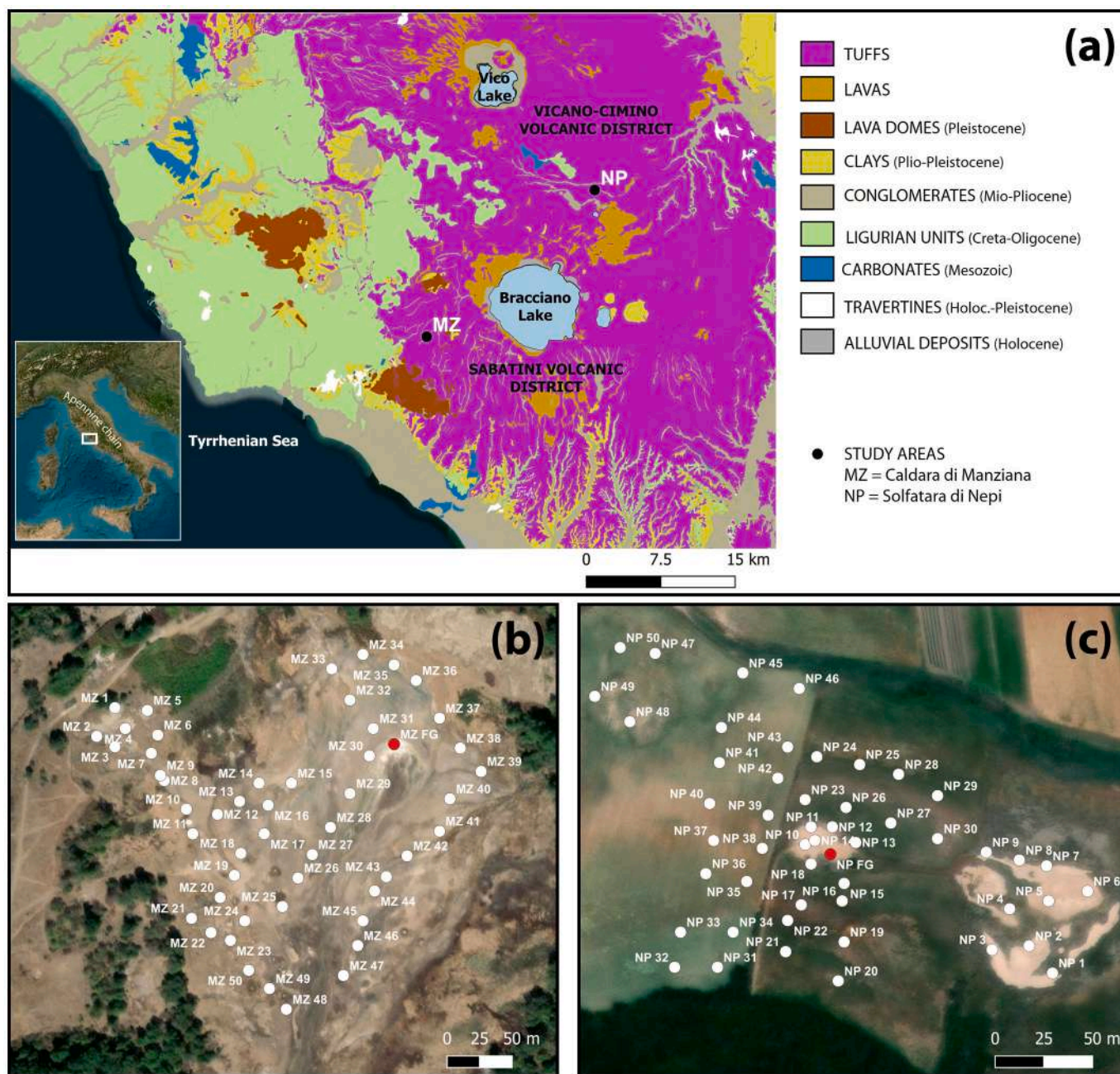


Fig. 1. (a) Location of the study areas in Central Italy; (b) selected sites for gas sampling (soil gases = white dots; free gases (FG) = red dots) and flux measurements at MZ; (c) selected sites for gas sampling (soil gases = white dots; free gases (FG) = red dots) and flux measurements at NP.

analyses.

Inorganic gases in both vial (CO_2 , N_2 , O_2 , Ar) and flask headspace (N_2 , O_2 , Ar) were analyzed using a Shimadzu 15A gas chromatograph (GC) equipped with a thermal conductivity detector (TCD), whereas light hydrocarbons (C_1 - C_3) were determined by means of a Shimadzu 14A GC equipped with a flame ionization detector (FID), as detailed elsewhere (Tassi et al., 2015a). Carbon dioxide and H_2S in the alkaline solution of the flasks were determined as CO_3^{2-} and SO_4^{2-} by (i) titration and (ii) ion chromatography (IC) after oxidation with H_2O_2 , respectively (Tassi et al., 2015a). VOCs were determined using a Thermo Trace GC Ultra gas chromatograph coupled to a Thermo DSQ quadrupole mass spectrometer (GC-MS) after solid phase micro extraction (SPME), as described by Tassi et al. (2015b). Retention times and mass spectra were used to identify VOCs using the NIST05 mass spectra library (NIST, 2005) for comparison. Calibration curves for quantitative analyses were constructed based on an external standard calibration procedure using Accustandard® standard mixtures in methanol or, alternatively, hexane solvent (Tassi et al., 2012). Relative standard deviation (RSD), calculated from five replicate analyses of the standard mixtures, was <5 %. The limit of quantification (LOQ) was determined by linear extrapolation from the lowest standard used for the calibration curve adopting the area of a peak having a signal/noise ratio of 5.

3.2. Data analysis

Data analysis was carried out using R and R studio (R Core Team, 2021). Robust-PCA (Principal Component Analysis) was performed using the “robCompositions” R-package (Templ et al., 2011), after rounded zeros imputation (Martin-Fernandez et al., 2012; Templ et al., 2016), transforming the compositional data with *ilr* (isometric log-ratio)-transformation and then they were back-transformed to *clr* (centered log-ratio) coefficients (Sauro Graziano et al., 2020). For each dataset, only species with missing values <30 % were considered. Hierarchical clustering of compositional parts was performed based on Ward's method by using the “*clustCoDa_qmode*” function of the “robCompositions” package (Templ et al., 2008; Filzmoser et al., 2018).

4. Results

4.1. Free-gas discharges

The chemical composition of free-gas discharges from MZ and NP (Table S1) was largely dominated by CO_2 (≥ 990 %), followed by N_2 (around 6 %). The MZ free gas was enriched in CH_4 and H_2S (3.84 and 0.86 %, respectively) with respect to the NP free gas (0.63 and 0.42 %, respectively). On the other hand, the NP free gas was characterized by more abundant VOCs with respect to the MZ free gas (ΣVOCs : 14.6 and 5.08 ppm, respectively).

The organic fraction was dominated by alkanes, accounting for 83.7 and 63.7 % of total VOCs (ΣVOCs) in NP and MZ free gas, respectively (Fig. 2). At NP, aromatics represented the second most abundant functional group (9.3 % ΣVOCs), followed by cyclics and S-substituted compounds (2.91 and 1.97 %, respectively), whereas O-substituted and halogenated compounds cumulatively accounted for 2.1 % ΣVOCs (Fig. 2). At MZ, aromatics and S-substituted compounds represented 18.5 and 12.5 % ΣVOCs , respectively, followed by cyclics (2.5 % ΣVOCs). O-substituted and halogenated compounds cumulatively accounted for 2.1 and 2.6 % ΣVOCs at NP and MZ, respectively (Fig. 2). Alkenes (mainly methylpropene) were present at low concentrations, i. e. 0.04 and 0.14 % ΣVOCs at NP and MZ, respectively (Fig. 2).

Among C_{2+} alkanes, $\text{C}_{2,3}$ alkanes (i.e. ethane and propane) and n-hexane were the most abundant compounds in NP and MZ free gas (46.9 and 40.9 % ΣVOCs as a sum, respectively), n-hexane showing an enrichment in the NP free gas (Figs. 3a and 4). The $\text{C}_{4,5,7+}$ alkanes followed an overall decreasing trend in relative abundances at increasing molecular weight (Fig. 4). Aromatics were dominated by benzene (6.14

and 12.3 % ΣVOCs in NP and MZ free gas, respectively) with respect to alkylated aromatics (Fig. 3b). Among alkylated aromatics, toluene in the NP free gas (0.80 % ΣVOCs) and ethylbenzene in the MZ free gas (1.30 % ΣVOCs) were the most abundant compounds. The NP and MZ free gases had cyclohexane and cyclopentane as the most abundant cyclics, accounting for 1.75 and 1.36 % ΣVOCs in the NP free gas, and 0.93 and 1.00 % ΣVOCs in the MZ free gas, respectively (Fig. 3c). S-substituted species were dominated by dimethylsulfide and dimethylsulfoxide: 0.95 and 0.66 % ΣVOCs in the NP free gas, and 4.23 and 3.86 % ΣVOCs in the MZ free gas, respectively (Fig. 3d). The MZ free gas was enriched in thiophene with respect to the NP free gas (2.66 and 0.23 % ΣVOCs , respectively; Fig. 3d). The halogenated compounds in both sites were mainly represented by trichloroethylene (0.03 and 0.10 % ΣVOCs at NP and MZ, respectively) and chlorohexane (0.02 and 0.08 % ΣVOCs at NP and MZ, respectively); carbon tetrachloride was enriched in the MZ free gas with respect to that collected at NP (0.07 and 0.01 % ΣVOCs , respectively). Among O-substituted species, aliphatic compounds mostly consisted of aldehydes (0.77 % ΣVOCs), followed by esters and ketones (0.19 and 0.18 % ΣVOCs , respectively), in the NP free gas and by esters and aldehydes (0.24 and 0.23 % ΣVOCs) with minor amounts of ketones (0.11 % ΣVOCs) in the MZ free gas; alcohols accounted for 0.10 and 0.02 % ΣVOCs in the NP and MZ free gases, respectively (Fig. 3e). Aromatic O-bearing compounds (phenol and benzaldehyde) cumulatively accounted for 0.82 and 1.68 % ΣVOCs in NP free gas and MZ free gas, respectively (Fig. 2f), phenol representing the most abundant aromatic O-bearing compound (0.66 and 1.59 % ΣVOCs in the NP and MZ free gases, respectively; Fig. 3f).

4.2. Diffuse soil fluxes

The measured soil CO_2 fluxes (Table S1) varied from 8.20 to 4980 $\text{g m}^{-2} \text{d}^{-1}$ at MZ (mean: 735.5 $\text{g m}^{-2} \text{d}^{-1}$; median: 208.0 $\text{g m}^{-2} \text{d}^{-1}$), whereas they ranged from 28.5 to 8200 $\text{g m}^{-2} \text{d}^{-1}$ at NP (mean: 1008 $\text{g m}^{-2} \text{d}^{-1}$; median: 365 $\text{g m}^{-2} \text{d}^{-1}$). The soil CH_4 fluxes (Table S1) were positively correlated to those of CO_2 and ranged from 0.0006 to 10.3 $\text{g m}^{-2} \text{d}^{-1}$ and from 0.0004 to 0.27 $\text{g m}^{-2} \text{d}^{-1}$ at MZ and NP, respectively (mean: 0.345 and 0.021 $\text{g m}^{-2} \text{d}^{-1}$, respectively; median: 0.0084 and 0.0039 $\text{g m}^{-2} \text{d}^{-1}$, respectively).

4.3. Soil gases

The collected soil gases displayed variable chemical compositions, ranging from N_2 - to CO_2 -dominated (Table S1). The contents of N_2 (from 15.9 to 840 % at MZ and from 15.0 to 771 % at NP) were positively correlated to O_2 (from 2.13 to 215 % at MZ and from 3.32 to 216 % at NP; Fig. S1a) and Ar (from 0.19 to 10.0 % at MZ and from 0.18 to 9.80 % at NP; Fig. S1b) and inversely correlated to CO_2 (from 36.4 to 979 % at MZ and from 58.7 to 980 % at NP; Fig. S1c). The CH_4 content (from 0.085 to 0.894 % at MZ and from 0.002 to 0.349 % at NP) similarly decreased as the concentrations of atmospheric-related species (i.e., N_2 , O_2 and Ar) increased (Fig. S1d). Accordingly, while the N_2 , O_2 and Ar contents increased approaching the soil-atmosphere interface, CO_2 and CH_4 concentrations were generally higher at 40 cm depth. The total organic fraction (ΣVOCs) varied from 81.6 to 2543 ppb at MZ, with higher concentrations at 40 cm depth with respect to the shallower samples (mean values: 1017 ppb at 40 cm, 606 ppb at 20 cm). Similarly, at NP ΣVOCs ranged from 86.3 to 6175 ppb at 20 cm depth and from 171 to 7046 ppb at 40 cm depth. The relative abundances, expressed as % ΣVOCs , of the measured organic functional groups in soil gases from MZ and NP are summarized in Fig. 2. Alkanes represented the dominant functional group, with mean relative abundances of 57 and 63 % ΣVOCs at 20 and 40 cm depth, respectively, at MZ and of 75 and 80 % ΣVOCs at 20 and 40 cm depth, respectively, at NP (Fig. 2a). Aromatics accounted for ca. 27 and 15 % ΣVOCs at MZ and NP, respectively, showing a slight increase at shallower depths (Fig. 2b). A similar trend was observed for both aliphatic and aromatic O-bearing species (Fig. 2e,f) and, to a lesser

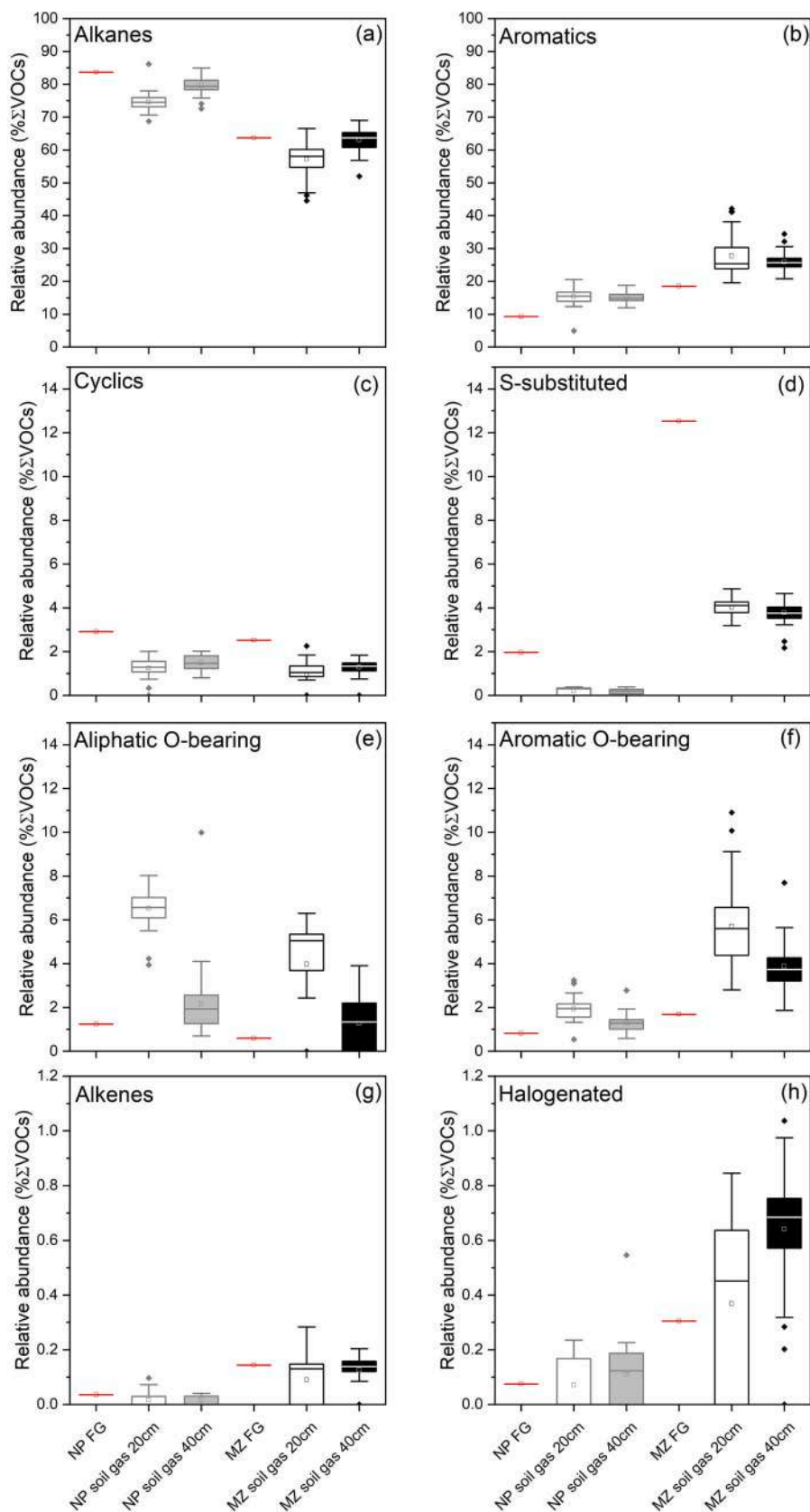


Fig. 2. Boxplots of relative abundances (expressed as %ΣVOCs) of (a) alkanes, (b) aromatics, (c) cyclics, (d) S-substituted species, (e) aliphatic O-bearing compounds, (f) aromatic O-bearing compounds, (g) alkenes and (h) halogenated species in free gases (FG) and soil gases collected at 20 and 40 cm depth from MZ and NP. Each box stretches from the first to the third quartile (Q1 and Q3, respectively), i.e. showing the interquartile range (IQR). The median value is marked by the line that divides each box, whereas the mean value is depicted as an open square symbol. The whiskers represent samples lying within 1.5 times the IQR. Outliers (i.e. values that are $>1.5 \times$ IQR below Q1 or below Q3) are marked with diamond symbols.

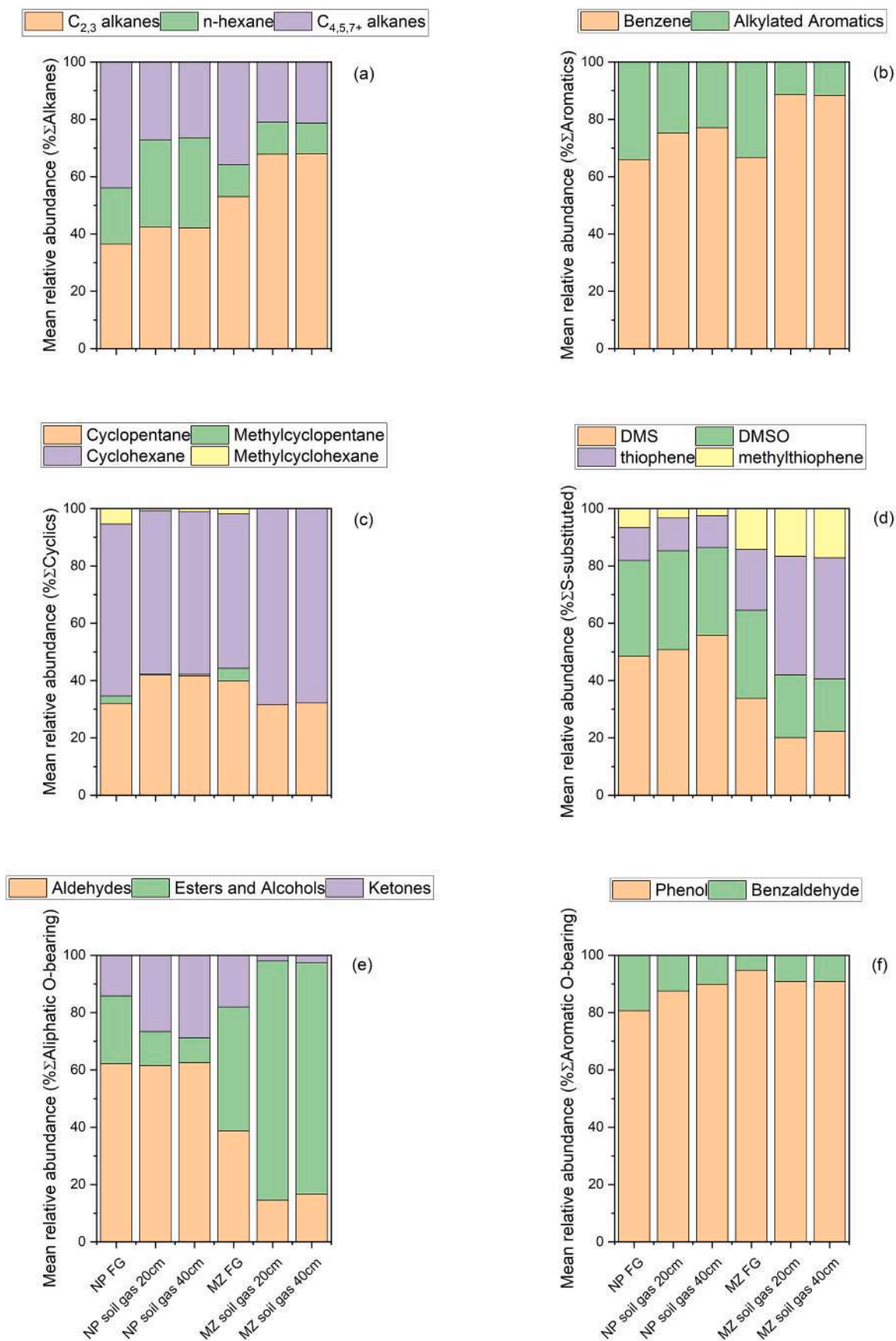


Fig. 3. 100 % stacked bar charts showing mean composition of (a) alkanes, (b) aromatics, (c) cyclics, (d) S-substituted species, (e) aliphatic O-bearing compounds and (f) aromatic O-bearing compounds in free gases (FG) and soil gases collected at 20 and 40 cm depth from MZ and NP.

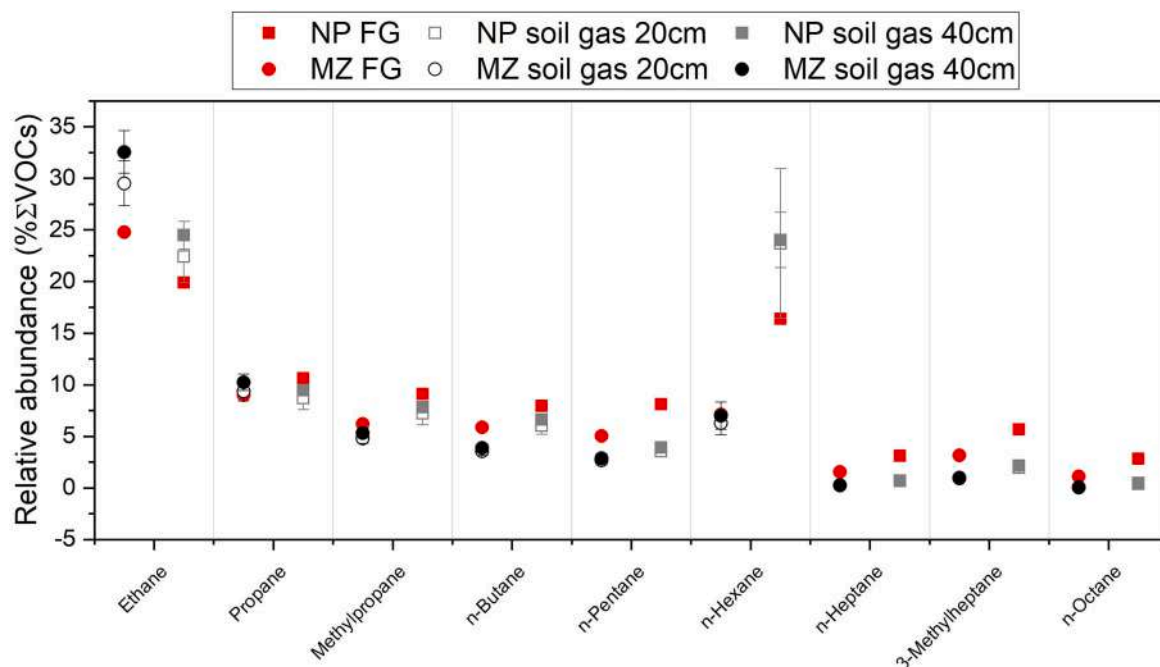


Fig. 4. Relative abundances (mean values and standard deviation, expressed as %ΣVOCs) of alkanes in free gas (FG) and soil gas samples from MZ and NP.

extent, S-substituted compounds (Fig. 2d). Differently, the relative abundances of cyclics were, on average, higher at 40 cm depth with respect to 20 cm depth.

The most abundant organic compound was ethane, accounting for 30 and 33 % ΣVOCs (median values) at 20 and 40 cm depth at MZ and for 23 and 25 % ΣVOCs (median values) at 20 and 40 cm depth at NP. At MZ, ethane was followed, in order of decreasing median relative abundances, by benzene (ca. 23 % ΣVOCs at both depths), propane (ca. 10 % ΣVOCs at both depths), n-hexane (ca. 7 % ΣVOCs at both depths), methylpropane (ca. 5 % ΣVOCs at both 20 and 40 cm depth) and phenol (5.1 and 3.4 % ΣVOCs at 20 and 40 cm depth, respectively). At NP, ethane was followed, in order of decreasing median relative abundances, by n-hexane (22 and 23 % ΣVOCs at 20 and 40 cm depth), benzene (ca. 12 % ΣVOCs), propane (8.9 and 9.6 % ΣVOCs at 20 and 40 cm depth), methylpropane (7.4 and 7.9 % ΣVOCs at 20 and 40 cm depth) and n-butane (6.1 and 6.7 % ΣVOCs at 20 and 40 cm depth). The other species were detected at both sites at subordinate abundances with median values < 4 % ΣVOCs. The relative abundances of alkanes in the MZ and NP soil gases mirrored the pattern of the corresponding free gases, with C_{2,3} alkanes and n-hexane cumulatively accounting for ≥45%ΣAlkanes at both 20 and 40 cm depth (Fig. 3a) and C_{4,5,7+} alkanes (except for n-hexane) displaying decreasing abundances at increasing molecular weight (Fig. 4). C_{4,5,7+} alkanes were enriched in the NP soil gases with respect to those from MZ, particularly in those collected at 40 cm depth, with the largest increases being related to methylpropane and n-butane (Fig. 4). Interestingly, this general trend was not mirrored by ethane and propane, which were depleted in the NP soil gases with respect to those collected at MZ (Figs. 3a, 4). Normal-hexane deviated from the overall decreasing trend in relative abundances at increasing molecular weight (Fig. 4), showing a sharp enrichment with respect to shorter alkanes and relative abundances nearly 5 times higher at NP than MZ. Although benzene largely dominated among aromatics, the NP soil gases were enriched in alkylated aromatics with respect to the MZ soil gases (Fig. 3b). Among cyclics, cyclohexane was enriched in the NP soil gases with respect to MZ soil gases (Fig. 3c). A distinct speciation of the S-substituted species among the two study areas was observed, with thiophene and methylthiophene being enriched in the MZ soil gases with respect to those collected at NP, which, in turn, were dominated by dimethylsulfide (DMS) and dimethylsulfoxide (DMSO) (Fig. 3d). Among

O-bearing species, the relative abundances of aliphatic compounds ranged from 3.94 to 8.02 and from 0.69 to 9.99 % ΣVOCs at 20 and 40 cm depth at NP, whereas at MZ they were detected in 71 % of the analyzed samples with abundances ≤6.30 and ≤3.91 % ΣVOCs at 20 and 40 cm depth at MZ (Fig. 2e). The NP soil gases were enriched in aldehydes and ketones at both 20 and 40 cm depth with respect to those from MZ, the latter being enriched in esters (Fig. 3e). The aromatic O-bearing compounds (i.e. phenol and benzaldehyde) ranged from 0.54 to 3.24 and from 0.59 to 2.78 % ΣVOCs at 20 and 40 cm depth, respectively, at NP and from 2.81 to 10.90 and from 1.86 to 7.69 % ΣVOCs at 20 and 40 cm depth, respectively, at MZ (Fig. 2f), being mainly represented by phenol in both study areas (Fig. 3f).

5. Discussion

5.1. Insights into fluid sources and pathways

As highlighted in the previous section, free-gas discharges from MZ and NP have distinct geochemical features. The NP free gas displays relative enrichments in CO₂ and ΣVOCs with respect to the MZ free gas. On the other hand, CH₄ and H₂S are more abundant in the MZ free gas (Table S1). These features are in agreement with previous studies carried out on the SVD and VCVD hydrothermal manifestations (Cinti et al., 2014, 2017) and ascribed to increasing secondary processes affecting deep-sourced fluids moving from the western to the eastern sector of the peri-Tyrrhenian area of Central Italy. Specifically, the interaction of deep fluids with groundwater is likely responsible for the relatively low H₂S concentration in the NP free gas with respect to that of the MZ free gas, due to dissolution and oxidation processes during interaction with oxygenated groundwaters. Higher H₂S concentrations in the MZ free gas with respect to that of NP free gas imply a higher sulfur fugacity (Tassi et al., 2010), thus explaining the enrichment in S-substituted VOCs found in the MZ free gas (Fig. 2). Significant differences are also recognized when the concentrations of the different groups of VOCs are compared. For example, the alkenes to alkanes and the aromatics to alkanes ratios are higher in the MZ free gas (0.0023 and 0.29, respectively) with respect to those in the NP free gas (0.0004 and 0.11, respectively; Fig. S2a), in agreement with the relatively high temperatures of the MZ hydrothermal source with respect to that of NP (Cinti

et al., 2011), since dehydrogenation and/or dehydrocyclization reactions and subsequent aromatization are favored at increasing temperatures (Venturi et al., 2017). The higher cyclohexane/benzene and hexane/cyclohexane ratios observed in the NP free gas with respect to those characterizing the MZ free gas (0.28 and 0.11, respectively; Fig. S2b) also confirm the occurrence of lower temperature conditions at NP (Venturi et al., 2017). On the other hand, the relative enrichment in alkanes (Fig. 2a), aliphatic O-bearing compounds (in particular, aldehydes, ketones and alcohols; Figs. 2e, 3e), and the relatively low abundances of alkenes in the NP free gas (Fig. 2g) suggest the influence of more oxidizing conditions induced by the availability of oxygen supplied by enhanced interaction between deep fluids and circulating groundwater with respect to the MZ free gas. These findings are in agreement with previous chemical data and isotopic data in N_2 from gas emissions from the eastern sector of the peri-Tyrrhenian area of Central Italy, which evidenced a higher contribution from air with respect to the western sector (Cinti et al., 2017).

5.2. Hypogenic signature vs. shallow secondary processes from soil gases

The geochemical composition of soil gases collected from both MZ and NP was characterized by a relatively wide variability. The robust-PCA performed considering the main gaseous compounds (CO_2 , N_2 , O_2 , Ar, CH_4) and $\Sigma VOCs$ reveals that the first two principal components (PC1 and PC2) describe 91.7 % and 6.3 % of the whole dataset variability, respectively (Fig. 5a).

PC1 is largely dominated by CH_4 and inversely correlated with atmospheric gas species (N_2 , O_2 , Ar). Interestingly, PC1 governs the compositional variability of soil gases within each study area. As expected, hierarchical clustering of compositional parts (Fig. 5b) distinguishes two groups among the investigated variables: (i) the first group, represented by O_2 , N_2 , Ar, is related to the atmospheric contributions, and (ii) the second group, characterized by CH_4 , CO_2 and VOC, is related to deep-sourced fluids. As shown in Fig. 5a, soil gases stretch from the

gas discharge end-member towards progressive enrichments in atmospheric-derived species along PC1. Accordingly, PC1 describes the atmospheric vs. hypogenic contributions, which largely shapes the chemical composition of soil gases in the study areas, regardless of the sampling depth. Consistently, the CO_2 and CH_4 fluxes roughly show increasing trends as the PC1 values increase (Fig. S3), confirming the progressive contribution from the deep-sourced fluids. On the other hand, a clear distinction between the soil gases collected from the two study areas is evidenced along PC2, which is correlated with CH_4 and (inversely) with $\Sigma VOCs$, as also observed for the free-gas discharges (Fig. 5a). This observation testifies that soil gases are able to preserve distinct compositional information on the deep-sourced gas despite the occurrence of mixing processes with air and secondary chemical modifications occurring at shallow depths.

To investigate the VOC speciation in the collected soil gases and its response to changing environmental conditions within the soil and, hence, identify potential geochemical tracers of deep reservoir conditions, a further robust-PCA was performed considering the deep-sourced components, i.e., CH_4 , CO_2 and VOCs. Based on the overall compositional features of the organic fraction in soil gases (Figs. 2, 3 and 4), the following groups of VOCs were considered: $C_{2,3}$ alkanes, n-hexane, $C_{4,5,7+}$ alkanes (except for n-hexane), cyclics, benzene, alkylated aromatics, benzaldehyde, phenol, S-bearing compounds and aliphatic O-bearing species (alcohols, esters, aldehydes and ketones). Alkenes and halogenated compounds were not included due to their scattered presence. The soil gas samples characterized as being below the detection limits of alkenes and halogenated compounds accounted for 55 and 46 %, respectively, at NP and 27 and 19 % at MZ, respectively. The results of the robust-PCA are shown in Fig. 6a.

PC1, describing 83.3 % of the whole dataset variability, is directly correlated with n-hexane and inversely correlated with S-bearing species and CH_4 . The two study areas are clearly differentiated by PC1, the MZ soil gases showing enrichment in the S-bearing species. This feature is displayed by all soil gases collected at MZ, regardless of the hypogenic

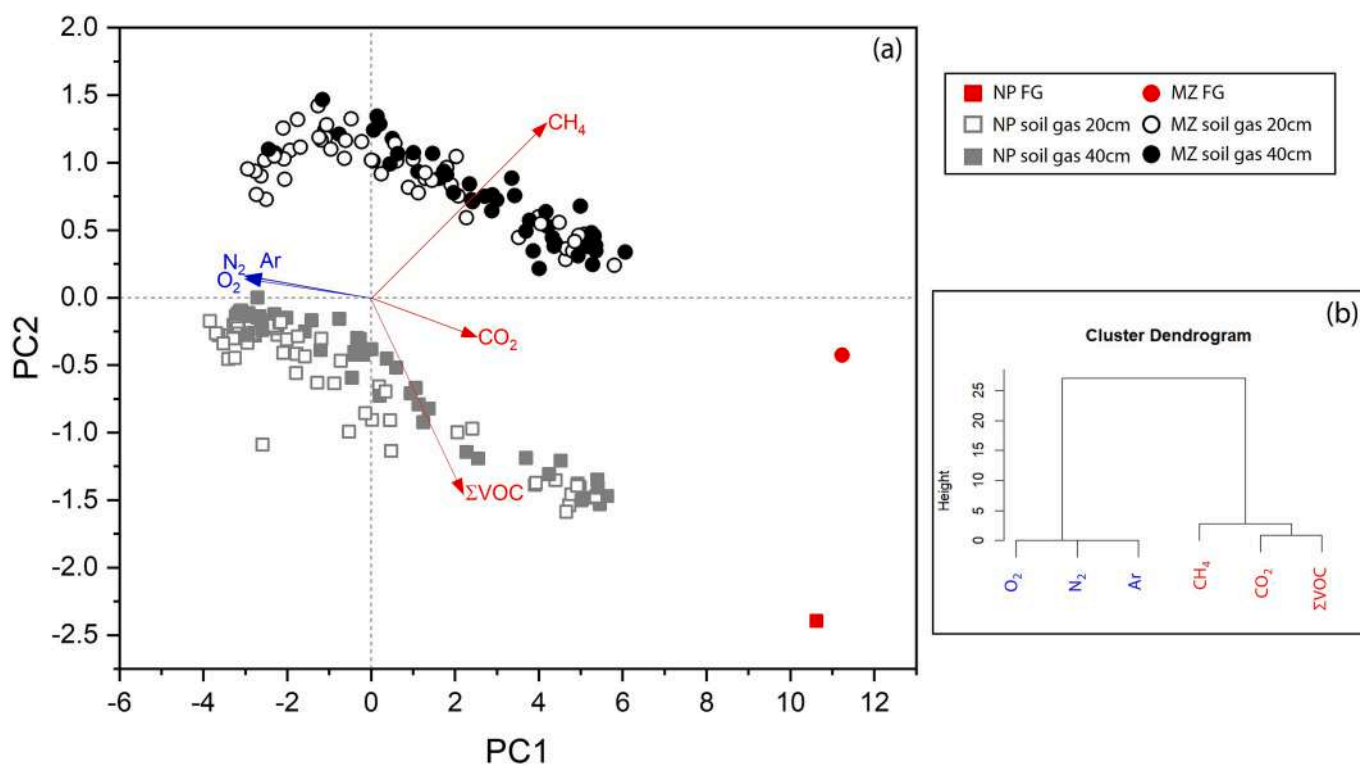


Fig. 5. (a) Robust-PCA performed on gas samples from MZ and NP considering the main gaseous compounds (CO_2 , N_2 , O_2 , Ar, CH_4) and the cumulative concentrations of VOCs ($\Sigma VOCs$). Symbol shapes and colors are detailed in the legend. (b) Dendrogram from hierarchical clustering of CO_2 , N_2 , O_2 , Ar, CH_4 and $\Sigma VOCs$ performed on the collected gas samples.

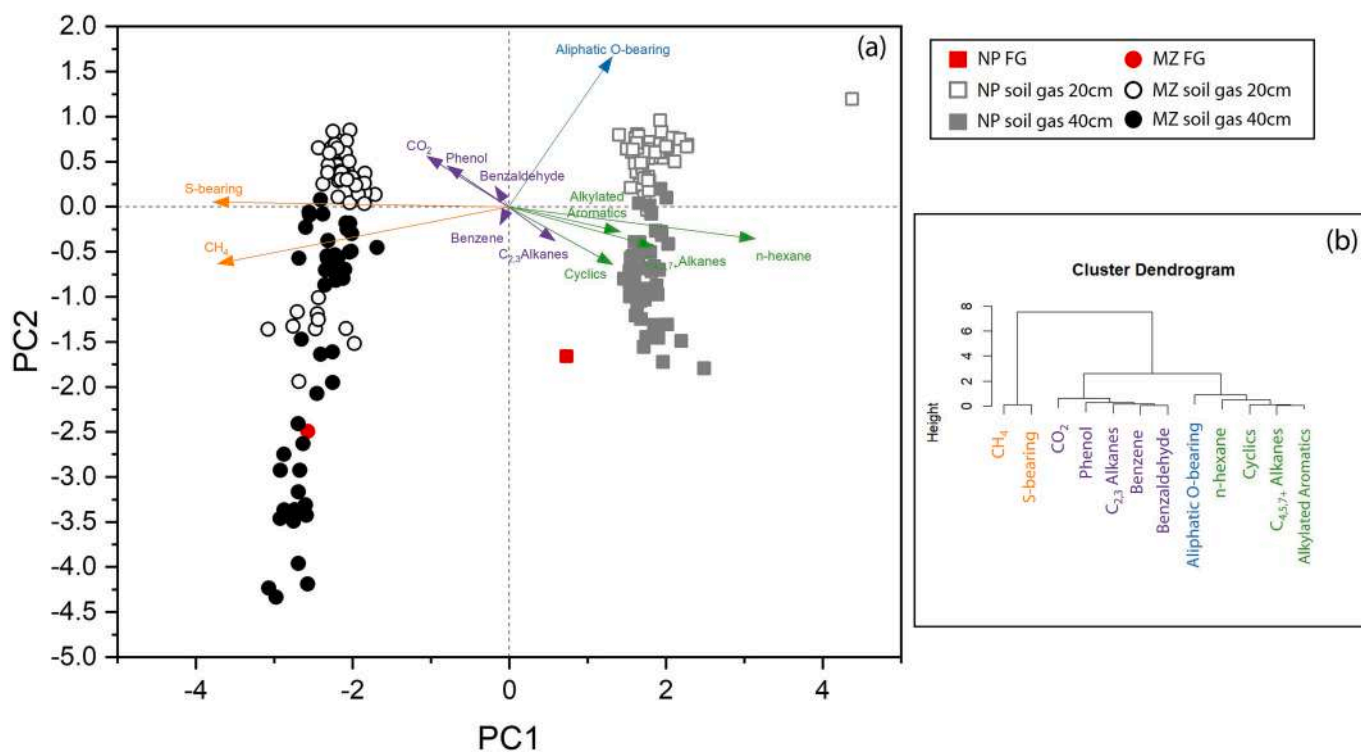


Fig. 6. (a) Robust-PCA performed on gas samples from MZ and NP considering CO_2 , CH_4 and concentrations of organic compounds ($\text{C}_{2,3}$ alkanes, n-hexane, $\text{C}_{4,5,7+}$ alkanes, cyclics, benzene, alkylated aromatics, benzaldehyde, phenol, S-bearing compounds and aliphatic O-bearing species). Symbol shapes and colors are detailed in the legend. (b) Dendrogram from hierarchical clustering of CO_2 , CH_4 and concentrations of organic compounds ($\text{C}_{2,3}$ alkanes, n-hexane, $\text{C}_{4,5,7+}$ alkanes, cyclics, benzene, alkylated aromatics, benzaldehyde, phenol, S-bearing compounds and aliphatic O-bearing species) performed on the collected gas samples.

vs. atmospheric contribution, suggesting that, at a first approximation, this compositional feature, inherited by the deep-sourced gas, was not eliminated by secondary processes at shallow depths nor affected by air contamination. On the other hand, the compositional variability of the soil gases from each site is governed by PC2 (accounting for 8.1 % of the whole dataset variability), which is strongly correlated with the aliphatic O-bearing compounds. Interestingly, a clear separation of soil gases collected from 20 and 40 cm depths is observed in Fig. 6a. The relative enrichment in the aliphatic O-bearing species, characterizing the shallowest soil portion, appears to be independent of the ratio between hypogenic and atmospheric contribution affecting soil gases. The origin of these organic compounds thus relates to ubiquitous secondary processes affecting the soil gases approaching the soil-atmosphere interface and likely supported by the increasing O_2 availability (Table S1). Overall, the distribution of soil gases collected from the two study areas shown in Fig. 6a reflects the compositional features of the respective free gases, evidencing the capability of the organic fraction of soil gases to preserve information on the hypogenic feeding source and allowing investigation of VOC speciation in soil gases as a potential geochemical tracer of the physicochemical conditions of the deep hydrothermal reservoir.

The hierarchical clustering of compositional parts (Fig. 6b) allowed assembly of the considered VOCs into four groups, implying distinct sources/sinks/geochemical behaviors: (i) S-bearing compounds, associated with CH_4 , (ii) $\text{C}_{4,5,7+}$ alkanes, n-hexane, cyclics and alkylated aromatics, (iii) $\text{C}_{2,3}$ alkanes, benzene, benzaldehyde, and phenol, related to CO_2 , and (iv) aliphatic O-bearing compounds. In the following sections, each group is discussed in order to evaluate the information provided by VOCs about the features of the feeding hydrothermal system.

5.2.1. S-bearing compounds

The abundance of S-bearing compounds governs the compositional

variability of soil gases between the two study areas and reflects the differences among the respective free gases (Fig. 6a). Accordingly, these compounds are directly influenced by the physicochemical features of the feeding systems, being enriched at increasing temperature and sulfur fugacity. The relative abundances of (i) thiophene and methylthiophene (Σ thiophenes) and (ii) DMS and DMSO (Fig. 3d) in soil gases are similarly controlled by the feeding source, with the Σ thiophenes/(DMS + DMSO) ratios (1.61 at MZ and 0.35 at NP) increasing at increasing reservoir temperature and sulfur fugacity, and rather constant within each study area (Fig. 7a), i.e. not significantly influenced by shallow processes. Accordingly, the Σ thiophenes/(DMS + DMSO) ratio in soil gases appears to be a suitable geochemical tracer for geothermal exploration. The overall enrichment in thiophenes observed in the MZ soil gases compared to those collected from NP is in agreement with a feeding source characterized by higher temperatures, as evidenced by the compositional features of the free-gas discharges, and by a larger availability of aromatics and metal sulfide catalysts (Madsen et al., 2015 and references therein; Venturi et al., 2017; Geisberger et al., 2021). On the other hand, the enrichment in DMS + DMSO in the NP soil gases with respect to those from MZ suggests that their origin is likely requiring lower temperatures with respect to thiophenes and favored by the larger availability of CH_4 (Madsen et al., 2015 and references therein). The DMS/DMSO ratio in soil gases is largely variable within each study area (Fig. 7b) showing (i) enrichments in DMS with respect to the MZ and NP free-gas discharges, suggesting that this compound might further be produced during relatively slow circulation of hydrothermal fluids at depth, e.g., due to prolonged interaction of organic compounds with H_2S or sulfide minerals or degradation of buried S-bearing organic matter (Sánchez-Avila et al., 2021; Randazzo et al., 2022) and (ii) enrichments in DMSO in the soil gases at 20 cm depth than those collected at 40 cm depth, pointing to the occurrence of shallow oxidative secondary processes (e.g., Schäfer et al., 2010; Eyice et al., 2015; Randazzo et al., 2020).

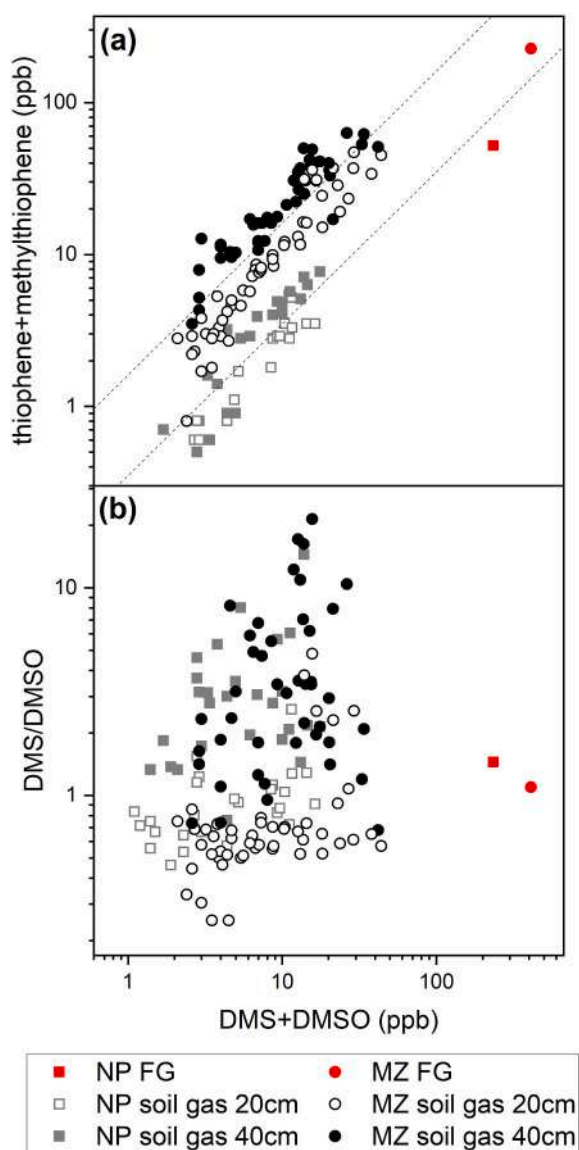


Fig. 7. Scatter plots of DMS + DMSO (in ppb) vs. (a) thiophene+methylthiophene (in ppb) and (b) DMS/DMSO ratio in gas samples from MZ and NP. The dashed lines in panel a correspond to the mean (thiophene+methylthiophene)/(DMS + DMSO) ratio in soil gases collected at MZ and NP.

5.2.2. $C_{4,5,7+}$ alkanes, *n*-hexane, cyclics and alkylated aromatics

These compounds have an opposite trend with respect to that shown by S-substituted species, being relatively enriched in the NP soil gases than in those from MZ (Fig. 6a). They are recognized as temperature-sensitive compounds, undergoing thermal degradation at increasing temperature conditions. Accordingly, the observed decreasing trend in alkane relative abundances at increasing molecular weight (Fig. 4), as observed in other hydrothermal systems (e.g., Tassi et al., 2015a; Venturi, 2017), is ascribed to the thermal degradation of organic matter (Darling, 1998). Longer-chain alkanes are indeed characterized by lower thermal stability (higher Gibbs energy of formation). Hence, the $C_{4,5,7+}$ depletion in the MZ soil gases may be due to the higher reservoir temperatures characterizing this area with respect to those from NP. The deviation of *n*-hexane relative abundances from this general pattern (Fig. 4) observed at both MZ and NP, in line with previous studies on several volcanic and hydrothermal systems, is attributed to the stability of the *n*-hexane structure and ongoing aromatization processes (e.g., Darling, 1998; Tassi, 2004; Venturi, 2017). In fact, *n*-hexane is expected

to be an intermediate product of dehydrocyclization and aromatization of longer alkanes together with cyclohexane (Venturi, 2017). Accordingly, the higher *n*-hexane/cyclohexane and cyclohexane/benzene ratios in soil gases from NP with respect to those from MZ (Fig. S2b), reflecting the compositional features of the respective free gases, is likely the result of an incomplete conversion of both alkanes to cyclics and cyclics to aromatics, the two reactions being increasingly impeded at decreasing temperatures (Venturi et al., 2017). Although cyclohexane is relatively depleted in the soil gases with respect to the corresponding free-gas discharges at both MZ and NP (Fig. S2b), likely due to a relatively high reactivity of cyclohexane during fluid circulation at depth, the differences in the *n*-hexane/cyclohexane and cyclohexane/benzene ratios between the two study areas are preserved. On the other hand, the relative enrichment in *n*-hexane and benzene in soil gases with respect to the corresponding free gases is favored by the stability of these compounds. Benzene is commonly considered a recalcitrant compound, enriched in gas sources at relatively high temperatures (e.g., Capaccioni et al., 1993, 1995; Tassi et al., 2010; Venturi, 2017; Venturi et al., 2017) and produced by thermal degradation of alkylated aromatics (e.g. McCollom et al., 2001). Accordingly, a sharp increase in the benzene/alkylated aromatics ratio affects the MZ soil gases (mean value 7.74) when compared to that recorded in the MZ free-gas (2.00; Figs. 3b, 8a). The enrichment in the benzene/alkylated aromatics ratio in the NP soil gases (mean value 3.23) with respect to that in the gas discharge (1.94) is occurring to a lesser extent with respect to that of MZ (Figs. 3b, 8a). This suggests that the degradation of alkylated aromatics is likely favored under the higher temperature conditions characterizing MZ, where the presence of sulfur compounds might further catalyze organic reactions. In the soil, the benzene/alkylated aromatics ratio is rather constant despite the different hypogenic gas contribution, except for those soil gases displaying larger atmospheric contributions (Fig. 5a, Table S1), for which a relative depletion in the alkylated aromatics is observed at both MZ and NP. Hence, an enhanced degradation of these compounds can be invoked in the shallowest portion of the soil where air diffusion is likely favoring the occurrence of aerobic microbial activity (Weelink et al., 2010; Vogt et al., 2011). Accordingly, the relative abundances of this group of VOCs in soil gases are informative of reservoir temperature conditions and may provide valuable geochemical tracers, especially if soil gases at 40 cm depth are considered.

5.2.3. $C_{2,3}$ alkanes, benzene, benzaldehyde and phenol, associated with CO_2

This group of VOCs distinctly characterized neither MZ nor NP, their contribution to the overall compositional variability of gas samples collected from the two study areas being negligible with respect to other VOCs (Fig. 6a). They include rather stable species ($C_{2,3}$ alkanes and benzene), characterized by relatively high thermal stability and resistance to degradation processes (Capaccioni et al., 1993) and possibly produced by thermal degradation of other VOCs (e.g. longer alkanes and alkylated aromatics). They are associated with hierarchical clustering (Fig. 6b) to phenol and benzaldehyde, indicating that sources or behaviors of the aromatic O-bearing compounds are similar. Interestingly, hierarchical clustering revealed that aromatic O-bearing compounds are not closely associated with aliphatic O-bearing compounds (Fig. 6b). Phenol was the most abundant O-bearing compound detected in the free-gas discharges, accounting for 70 % and 32 % of Σ O-bearing species at MZ and NP, respectively, suggesting a deep origin within the hydrothermal reservoir. Similar relative abundances with respect to the free gases were observed in NP and MZ soil gases (65 and 28 % of Σ O-bearing species at MZ and NP, respectively). Phenol was recognized as a byproduct of thermal degradation of C_6 cyclic hydrocarbons (Venturi et al., 2017) and oxidative decarboxylation of alkylated aromatics (McCollom et al., 2001). The higher phenol/cyclohexane and phenol/alkylated aromatics ratios measured in the MZ free-gas (1.17 and 0.26, respectively) than those registered in the NP free gas (0.38 and 0.21, respectively) (Fig. 8b,c) suggest that the higher temperatures

characterizing MZ favored the production of phenol in the deep gas reservoir and support the hypothesis of a more intense thermal degradation of cyclics and alkylated aromatics. Similarly, benzaldehyde was indicated as a possible intermediate product in the conversion of toluene (and other alkylated aromatics) to benzene and phenol (McCullom et al., 2001). Interestingly, benzaldehyde shows an opposite behavior with respect to phenol in the free-gas discharges, with slightly higher benzaldehyde/benzene and benzaldehyde/alkylated aromatics ratios in the NP free gas (0.03 and 0.05, respectively) with respect to those measured in the MZ free gas (0.01 and 0.01, respectively; Fig. 8b,c). This behavior would suggest either (i) an incomplete conversion of alkylated aromatics to benzene due to lower temperature conditions or (ii) an enhanced production of benzaldehyde sustained by a larger interaction with shallow aquifers. While phenol is generally enriched in soil gases with respect to MZ and NP free-gas discharges, benzaldehyde shows similar relative abundances in the NP soil gases and free gas (Fig. S4) with roughly homogenous benzaldehyde/alkylated aromatics ratios (Fig. 8c). On the other hand, the MZ soil gases show higher benzaldehyde relative abundances and higher benzaldehyde/alkylated aromatics ratios with respect to the free-gas (Figs. S4, 8c). This behavior may be consistent with an enhanced decomposition of alkylated aromatics to benzene and benzaldehyde production in the presence of high concentrations of dissolved sulfur compounds and relatively oxidizing conditions as hypothesized by McCullom et al. (2001). On the other hand, at both MZ and NP, a clear increase in the phenol/alkylated aromatics ratio is evidenced in the soil gases at 20 cm depth with respect to those collected at 40 cm depth (Fig. 8b), which is coupled with an analogous increase in the phenol/benzene ratio (Fig. 8d). This trend confirms the occurrence of shallow aerobic degradation of alkylated aromatics likely driven by soil microbial communities (e.g., Weelink et al., 2010 and references therein) and resulting in an additional and shallow source of phenol. On the other hand, a less clear trend is found for the benzaldehyde/benzene ratio in the soil gases at 20 cm depth, which is only slightly enriched in benzaldehyde with respect to those collected at 40 cm depth, suggesting that this compound is produced at lower amounts by shallow processes with respect to phenol. Accordingly, the relative abundances of this group of VOCs are related to the extent of thermal degradation processes and are affected by shallow secondary processes. Hence, although sensitive to reservoir conditions, C_{2,3} alkanes, benzene, benzaldehyde and phenol in soil gases are regarded as less suitable as geochemical tracers.

5.2.4. Aliphatic O-bearing compounds

The aliphatic O-bearing compounds govern the compositional variability of the organic fraction in the soil gases from each study area, with a clear relative enrichment at 20 cm depth with respect to those at 40 cm depth (Figs. 3 and 5). This trend was previously observed in other hydrothermal areas and attributed to secondary processes due to microbially-driven degradation of other organic constituents, such as long chain alkanes, alkenes and alkylated aromatics, occurring within the soil (e.g., Tassi et al., 2015a, 2015b; Crognale et al., 2018; Venturi et al., 2019a). Accordingly, the aliphatic O-bearing species are enriched in the soil gases with respect to those measured in the free-gas discharges (Fig. 2e). Nevertheless, the aliphatic O-bearing VOCs, such as aldehydes, ketones, alcohols and esters, can also be formed as byproducts of abiotic reactions in lab experiments simulating hydrothermal conditions (e.g., Seewald, 2001, 2003; Shipp et al., 2013; Venturi et al., 2017) and they were also detected in the MZ and NP free-gas samples (Table S1). This implies that an additional source, related to the direct contribution of deep-origin fluids, has to be considered. Moreover, as shown in Fig. 3e, compositional differences are observed between free-gas discharges and soil gases from NP and MZ, suggesting that, despite their shallow additional production in the soil, these compounds may carry information about the deep conditions and fluid circulation dynamics. Alcohols were detected at low amounts in the study areas. Accordingly, although these compounds are easily produced through the hydration of alkenes (Seewald, 2001, 2003), a process that is

thermodynamically enhanced at decreasing temperatures (Shock et al., 2013), their reactivity under hydrothermal conditions was experimentally observed to be even higher than that of alkenes (Shipp et al., 2013). Hence, unless a rapid uprising of hydrothermal fluids able to quench the chemical features of the deep reservoirs up to the surface occurs, alcohols are expected to undergo secondary processes, such as dehydrogenation to aldehydes and ketones, or reactions with carboxylic acids forming esters (Shock et al., 2013). Esters dominate the composition of the aliphatic O-bearing species at MZ (Fig. 3e), their production being likely supported by the availability of potential catalysts (e.g., sulfuric acid due to the interaction between H₂S and shallow aquifers). Moreover, the production of carboxylic acids by oxidation of n-alkanes has experimentally been observed (Seewald, 2001). On the other hand, the large occurrence of aldehydes and ketones at NP (Fig. 3e) suggests that the production of these compounds can be supported by extensive interaction with groundwaters.

Thus, although affected by secondary processes at shallow depths, the speciation of aliphatic O-bearing species in soil gases apparently preserves information on fluid circulation dynamics and conditions of the feeding reservoir. Hence, their potentiality in terms of geochemical tracers deserves further investigations.

6. Conclusions

The primary goal of this study was to investigate the capability of soil gases from diffuse degassing hydrothermal areas to bear information about the pristine chemical composition of the organic fraction of the deep-sourced feeding fluids, the latter being represented by the chemical features of the free-gas discharges. The comparison of soil gas samples from two hydrothermal systems, characterized by diverse compositions of the uprising hydrothermal fluids, revealed that, despite the occurrence of some chemical modifications induced by very shallow processes in the soil, the organic fraction of soil gases reflects the compositional dissimilarities of the free-gas discharges from Caldara di Manziana (MZ) and Solfatara di Nepi (NP). According to our results, the VOC speciation in soil gases collected from hydrothermal areas can be regarded as a powerful geochemical tracer, being able to track physicochemical dissimilarities of deep hydrothermal fluids even more efficiently than main gas species. Among VOCs, four distinct groups were recognized, each showing distinct features related to the characteristics of the feeding hydrothermal system, as summarized below.

- (i) S-bearing compounds (i.e., thiophenes, DMS, DMSO). These compounds govern the compositional dissimilarities in the VOC speciation between MZ and NP. The higher abundance of S-bearing compounds and the larger proportion of thiophenes at MZ reflect higher temperature conditions and larger sulfur availability of the hydrothermal source. Moreover, while thiophenes appear to be favored by a more direct connection with the deep reservoir, the production of DMS (and DMSO, as the relative oxidation product) is likely enhanced by lower temperatures and more extensive interaction of hydrothermal fluids with the available (e.g., metal sulfide) catalysts. Moreover, the DMS enrichment in soil gases affected by large hypogenic contributions with respect to the free-gas discharges indicates the occurrence of additional production of this compound as the hydrothermal fluids move to the surface through low and moderately permeable pathways. The relationship between Σthiophenes/(DMS + DMSO) ratios in soil gases and reservoir temperature conditions suggests that this ratio can be suitable as a geochemical tracer for geothermal exploration.
- (ii) C_{4,5,7+} alkanes, n-hexane, cyclics and alkylated aromatics. These compounds represent temperature-sensitive species that undergo thermal degradation at relatively high temperature conditions. Accordingly, they show an opposite trend with respect to S-bearing compounds, being enriched at decreasing reservoir

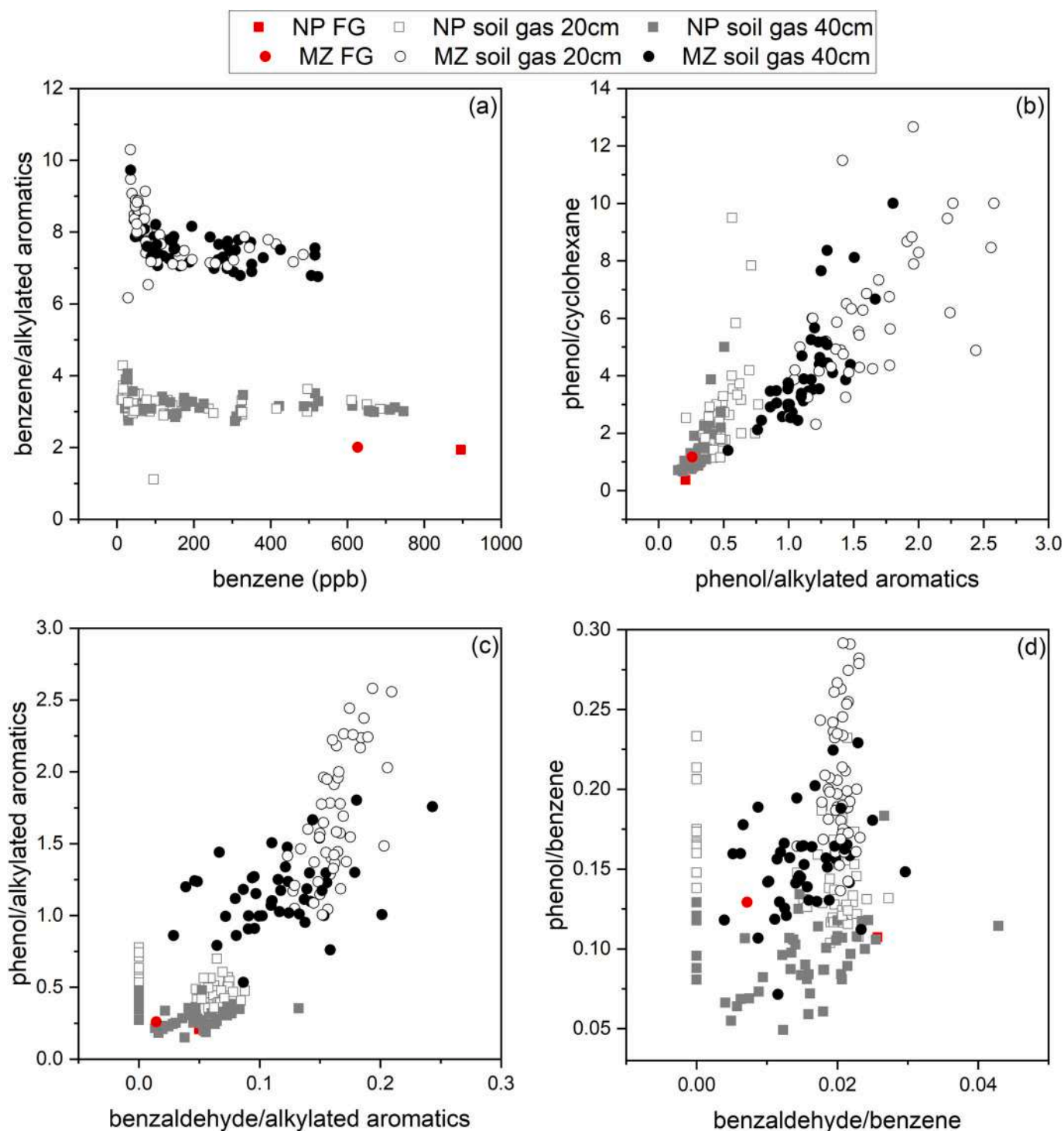


Fig. 8. Scatter plots of (a) benzene/alkylated aromatics ratio vs. benzene (in ppb), (b) phenol/cyclohexane ratio vs. phenol/alkylated aromatics, (c) phenol/alkylated aromatics ratio vs. benzaldehyde/alkylated aromatics ratio, and (d) phenol/benzene ratio vs. benzaldehyde/benzene ratio in free-gas (FG) and soil gas samples from MZ and NP.

temperature conditions. Together with S-substituted species, they can be regarded as valuable geochemical tracers.

- (iii) $C_{2,3}$ alkanes, benzene, benzaldehyde and phenol. This group of VOCs can be regarded as compounds directly fed by the deep hydrothermal system and additionally sustained by the degradation of other reactive VOCs during fluid circulation both at deep and shallow depths. Although sensitive to reservoir conditions, the use of these compounds in soil gases as geochemical tracers appears to be more challenging.

- (iv) Aliphatic O-bearing compounds (esters, alcohols, aldehydes, ketones). The sharp increase in the relative abundances of aliphatic O-bearing compounds from 40 to 20 cm depth indicates an active (likely microbially-driven) production of these compounds within the soil. However, the peculiar and distinct chemical speciation characterizing the two study areas highlights that the physicochemical conditions of the feeding systems and the modalities of the hydrothermal fluids uprising towards the surface are able to condition and maintain a signature of the relative

proportions of esters, aldehydes and ketones detected in the soil gases. Their potentiality as geochemical tracers requires further investigation.

Our results suggest that the chemical composition of the organic fraction from soil gases is a valuable tool to be applied in volcanic and geothermal environments. VOCs can indeed retrieve useful information on the physicochemical conditions of the deep hydrothermal reservoirs, backing up traditional methods based on the main gas species and diffuse soil flux measurements. Our approach is also particularly relevant for investigating (i) hidden hydrothermal systems where surface manifestations such as fumaroles, bubbling and boiling pools are missing, (ii) the spatial variations of physicochemical conditions of deep hydrothermal reservoirs, and (iii) heterogeneities in fluid circulation dynamics. The present field evidence provides a valuable framework for future experimental studies aimed at investigating the reaction mechanisms and environmental drivers controlling the occurrence and speciation of VOCs as important geochemical tracers.

Supplementary data to this article can be found online at <https://doi.org/10.1016/j.scitotenv.2023.169047>.

CRediT authorship contribution statement

Stefania Venturi: Conceptualization, Formal analysis, Investigation, Methodology, Software, Visualization, Writing – original draft. **Antonio Randazzo:** Conceptualization, Data curation, Writing – review & editing. **Jacopo Cabassi:** Investigation, Writing – review & editing. **Daniele Cinti:** Investigation, Visualization, Writing – review & editing. **Federica Meloni:** Investigation, Writing – review & editing. **Monia Procesi:** Investigation, Visualization, Writing – review & editing. **Barbara Nisi:** Investigation, Writing – review & editing. **Nunzia Voltattorni:** Investigation, Writing – review & editing. **Francesco Capecchiacci:** Conceptualization, Investigation, Writing – review & editing. **Tullio Ricci:** Investigation, Writing – review & editing. **Orlando Vaselli:** Investigation, Resources, Writing – review & editing. **Franco Tassi:** Conceptualization, Data curation, Resources, Supervision, Writing – review & editing.

Declaration of competing interest

The authors declare that they have no known competing financial interests or personal relationships that could have appeared to influence the work reported in this paper.

Data availability

Data will be made available on request.

Acknowledgments

The authors wish to thank the Italian Geochemical Society (So.Ge.I.) for partly supported the field activities. The Fluid Geochemistry, the Environmental Geochemistry and the Stable Isotopes laboratories of the Department of Earth Sciences (University of Florence) are gratefully acknowledged for covering the analytical expenses. K. Fecteau and other two anonymous reviewers are warmly acknowledged for their careful reading of the manuscript and their valuable and insightful comments and suggestions that contributed to improve the quality of our manuscript.

References

Abbasian, F., Lockington, R., Mallavarapu, M., Naidu, R., 2015. A comprehensive review of aliphatic hydrocarbon biodegradation by bacteria. *Appl. Biochem. Biotechnol.* 176, 670–699. <https://doi.org/10.1007/s12010-015-1603-5>.
 Capaccioni, B., Mangani, F., 2001. Monitoring of active but quiescent volcanoes using light hydrocarbon distribution in volcanic gases: the results of 4 years of

discontinuous monitoring in the Campi Flegrei (Italy). *Earth Planet. Sci. Lett.* 188, 543–555. [https://doi.org/10.1016/S0012-821X\(01\)00338-7](https://doi.org/10.1016/S0012-821X(01)00338-7).
 Capaccioni, B., Martini, M., Mangani, F., Giannini, L., Nappi, G., Prati, F., 1993. Light hydrocarbons in gas-emissions from volcanic areas and geothermal fields. *Geochem. J.* 27, 7–17. <https://doi.org/10.2343/geochemj.27.7>.
 Capaccioni, B., Martini, M., Mangani, F., 1995. Light hydrocarbons in hydrothermal and magmatic fumaroles: hints of catalytic and thermal reactions. *Bull. Volcanol.* 56, 593–600. <https://doi.org/10.1007/BF00301464>.
 Capaccioni, B., Tassi, F., Vaselli, O., 2001. Organic and inorganic geochemistry of low temperature gas discharges at the Baia di Levante beach, Vulcano Island, Italy. *J. Volcanol. Geotherm. Res.* 108, 173–185. [https://doi.org/10.1016/S0377-0273\(00\)00284-5](https://doi.org/10.1016/S0377-0273(00)00284-5).
 Cinti, D., Procesi, M., Tassi, F., Montegrossi, G., Sciarra, A., Vaselli, O., Quattrocchi, F., 2011. Fluid geochemistry and geothermometry in the western sector of the Sabatini Volcanic District and the Tolfa Mountains (Central Italy). *Chem. Geol.* 284, 160–181. <https://doi.org/10.1016/j.chemgeo.2011.02.017>.
 Cinti, F., Tassi, F., Procesi, M., Bonini, M., Capecchiacci, F., Voltattorni, N., Vaselli, O., Quattrocchi, F., 2014. Fluid geochemistry and geothermometry in the unexploited geothermal field of the Vicano-Cimino Volcanic District (Central Italy). *Chem. Geol.* 371, 96–114. <https://doi.org/10.1016/j.chemgeo.2014.02.005>.
 Cinti, D., Tassi, F., Procesi, M., Brusca, L., Cabassi, J., Capecchiacci, F., Delgado, Huertas A., Galli, G., Grassa, F., Vaselli, O., Voltattorni, N., 2017. Geochemistry of hydrothermal fluids from the eastern sector of the Sabatini Volcanic District (central Italy). *Appl. Geochem.* 84, 187–201. <https://doi.org/10.1016/j.apgeochem.2017.06.014>.
 Costa, A., Chiodini, G., Granieri, D., Folch, A., Hankin, R.K.S., Caliro, S., Avino, R., Cardellini, C., 2008. A shallow-layer model for heavy gas dispersion from natural sources: application and hazard assessment at Caldara di Manziiana, Italy. *Geochem. Geophys. Geosyst.* 9, Q03002 <https://doi.org/10.1029/2007GC001762>.
 Crognale, S., Venturi, S., Tassi, F., Rossetti, S., Rashed, H., Cabassi, J., Capecchiacci, F., Nisi, B., Vaselli, O., Morrison, H.G., Sogin, M.L., Fazi, S., 2018. Microbiome profiling in extremely acidic soils affected by hydrothermal fluids: the case of the Solfatara Crater (Campi Flegrei, southern Italy). *FEMS Microbiol. Ecol.* 94 (fiy190) <https://doi.org/10.1093/femsec/fiy190>.
 Darling, W.G., 1998. Hydrothermal hydrocarbon gases: 1, genesis and geothermometry. *Appl. Geochem.* 13 (7), 815–824. [https://doi.org/10.1016/S0883-2927\(98\)00013-4](https://doi.org/10.1016/S0883-2927(98)00013-4).
 Eyice, Ö., Namura, M., Chen, Y., Mead, A., Samavedam, S., Schäfer, H., 2015. SIP metagenomics identifies uncultivated Methylophilaceae as dimethylsulphide degrading bacteria in soil and lake sediment. *ISME J.* 9 (11), 2336–2348. <https://doi.org/10.1038/ismej.2015.37>.
 Filzmoser, P., Hron, K., Templ, M., 2018. *Applied Compositional Data Analysis*. Springer, Cham.
 Geisberger, T., Sobotta, J., Eisenreich, W., Huber, C., 2021. Formation of Thiophene under simulated volcanic hydrothermal conditions on earth—implications for early life on extraterrestrial planets? *Life* 11, 149. [10.3390/life11020149](https://doi.org/10.3390/life11020149).
 Hanson, R.S., Hanson, T.E., 1996. Methanotrophic bacteria. *Microbiol. Rev.* 60 (2), 439–471. <https://doi.org/10.1128/mr.60.2.439-471.1996>.
 Madsen, R.B., Christensen, P.S., Houlberg, K., Lappa, E., Mørup, A.J., Klemmer, M., Olsen, E.M., Jensen, M.M., Becker, J., Iversen, B.B., Glasius, M., 2015. Analysis of organic gas phase compounds formed by hydrothermal liquefaction of dried distillers grains with solubles. *Bioresour. Technol.* 192, 826–830. <https://doi.org/10.1016/j.biortech.2015.05.095>.
 Martín-Fernández, J.A., Hron, K., Templ, M., Filzmoser, P., Palarea-Albaladejo, J., 2012. Model-based replacement of rounded zeros in compositional data: classical and robust approaches. *Comput. Stat. Data Anal.* 56 (9), 2688–2704. <https://doi.org/10.1016/j.csda.2012.02.012>.
 McCollom, T.M., Seewald, J.S., Simoneit, B.R.T., 2001. Reactivity of monocyclic aromatic compounds under hydrothermal conditions. *Geochim. Cosmochim. Acta* 65 (3), 455–468. [https://doi.org/10.1016/S0016-7037\(00\)00533-0](https://doi.org/10.1016/S0016-7037(00)00533-0).
 Minissale, A., 2004. Origin, transport and discharge of CO₂ in central Italy. *Earth Sci. Rev.* 66, 89–141. <https://doi.org/10.1016/j.earscirev.2003.09.001>.
 NIST/EPA/NIH Mass Spectral, 2005. Library. <http://www.nist.gov/srd/nist1a.htm>.
 R Core Team, 2021. R: A Language and Environment for Statistical Computing. R Foundation for Statistical Computing, Vienna, Austria. <https://www.R-project.org/>.
 Ranaldi, M., Lelli, M., Tarchini, L., Carapezza, M.L., Patera, A., 2016. Estimation of the geothermal potential of the Caldara di Manziiana site in the Sabatini Volcanic District (central Italy) by integrating geochemical data and 3D-GIS modelling. *Geothermics* 62, 115–130. <https://doi.org/10.1016/j.geothermics.2016.04.003>.
 Randazzo, A., Asensio-Ramos, M., Melián, G.V., Venturi, S., Padrón, E., Hernández, P.A., Pérez, N.M., Tassi, F., 2020. Volatile organic compounds (VOCs) in solid waste landfill cover soil: chemical and isotopic composition vs. degradation processes. *Sci. Total Environ.* 726, 138326 <https://doi.org/10.1016/j.scitotenv.2020.138326>.
 Randazzo, A., Folino, A., Tassi, F., Tatano, F., Rosa, S., De Gambioli, A., 2022. Volatile organic compounds from green waste anaerobic degradation at lab-scale: evolution and comparison with landfill gas. *Detritus* 19, 63–74. <https://doi.org/10.31025/2611-4135/2022.15188>.
 Randazzo, A., Zorzi, F., Venturi, S., Biccocchi, G., Viti, G., Tatano, F., Tassi, F., 2023. Degradation of biogas in a simulated landfill cover soil at laboratory scale: compositional changes of main components and volatile organic compounds. *Waste Manag.* 157, 229–241. <https://doi.org/10.1016/j.wasman.2022.12.027>.
 Rogie, J.D., Kerrick, D.M., Chiodini, G., Frondini, F., 2000. Flux measurements of nonvolcanic CO₂ emission from some vents in central Italy. *J. Geophys. Res.* 105 (B4), 8435–8445. <https://doi.org/10.1029/1999JB900430>.
 Rojo, F., 2009. Degradation of alkanes by bacteria. *Environ. Microbiol.* 11 (10), 2477–2490. <https://doi.org/10.1111/j.1462-2920.2009.01948.x>.

- Sánchez-Avila, J.I., García-Sánchez, B.E., Vara-Castro, G.M., Kretzschmar, T., 2021. Distribution and origin of organic compounds in the condensates from a Mexican high-temperature geothermal field. *Geothermics* 89, 101980. <https://doi.org/10.1016/j.geothermics.2020.101980>.
- Sauro Graziano, R., Gozzi, C., Buccianti, A., 2020. Is Compositional Data Analysis (CoDA) a theory able to discover complex dynamics in aqueous geochemical systems? *J. Geochem. Explor.* 211, 106465 <https://doi.org/10.1016/j.gexplo.2020.106465>.
- Schäfer, H., Myronova, N., Boden, R., 2010. Microbial degradation of dimethylsulphide and related C₁-sulphur compounds: organisms and pathways controlling fluxes of sulphur in the biosphere. *J. Exp. Bot.* 61 (2), 315–334. <https://doi.org/10.1093/jxb/erp355>.
- Schwandner, F.M., Seward, T.M., Gize, A.P., Hall, A., Dietrich, V.J., 2004. Diffuse emission of organic trace gases from the flank and crater of a quiescent active volcano (Vulcano, Aeolian Islands, Italy). *J. Geophys. Res.* 109, D04301 <https://doi.org/10.1029/2003JD003890>.
- Schwandner, F.M., Seward, T.M., Gize, A.P., Hall, A., Dietrich, V.J., 2013. Halocarbons and other trace heteroatomic organic compounds in volcanic gases from Vulcano (Aeolian Islands, Italy). *Geochim. Cosmochim. Acta* 101, 191–221. <https://doi.org/10.1016/j.gca.2012.10.004>.
- Seewald, J.S., 2001. Aqueous geochemistry of low molecular weight hydrocarbons at elevated temperatures and pressures: constraints from mineral buffered laboratory experiments. *Geochim. Cosmochim. Acta* 65 (10), 1641–1664. [https://doi.org/10.1016/S0016-7037\(01\)00544-0](https://doi.org/10.1016/S0016-7037(01)00544-0).
- Seewald, J.S., 2003. Organic-inorganic interactions in petroleum-producing sedimentary basins. *Nature* 426, 327–333. <https://doi.org/10.1038/nature02132>.
- Shipp, J., Gould, I.R., Herckes, P., Shock, E.L., Williams, L.B., Hartnett, H.E., 2013. Organic functional group transformations in water at elevated temperature and pressure: reversibility, reactivity, and mechanisms. *Geochim. Cosmochim. Acta* 104, 194–209. <https://doi.org/10.1016/j.gca.2012.11.014>.
- Shock, E.L., Canovas, P., Yang, Z., Boyer, G., Johnson, K., Robinson, K., Fecteau, K., Windman, T., Cox, A., 2013. Thermodynamics of organic transformations in hydrothermal fluids. *Rev. Mineral. Geochem.* 76, 311–350. <https://doi.org/10.2138/rmg.2013.76.9>.
- Taran, Y.A., Giggensbach, W.F., 2003. Geochemistry of light hydrocarbons in subduction-related volcanic and hydrothermal fluids. In: Simmons, S.F., Graham, I. (Eds.), *Volcanic, Geothermal, and Ore-Forming Fluids: Rulers and Witnesses of Processes Within the Earth*. Society of Economic Geologists. Special Publication, no. 10, pp. 61–74.
- Tassi, F., 2004. *Fluidi in ambiente vulcanico: evoluzione temporale dei parametri composizionali e distribuzione degli idrocarburi leggeri in fase gassosa*. Doctoral thesis., University of Florence, Italy.
- Tassi, F., Martinez, C., Vaselli, O., Capaccioni, B., Viramonte, J., 2005a. Light hydrocarbons as redox and temperature indicators in the geothermal field of El Tatio (northern Chile). *Appl. Geochem.* 20, 2049–2062. <https://doi.org/10.1016/j.apgeochem.2005.07.013>.
- Tassi, F., Vaselli, O., Capaccioni, B., Giolito, C., Duarte, E., Fernandez, E., Minissale, A., Magro, G., 2005b. The hydrothermal-volcanic system of Rincon de la Veja volcano (Costa Rica): a combined (inorganic and organic) geochemical approach to understanding the origin of the fluid discharges and its possible application to volcanic surveillance. *J. Volcanol. Geotherm. Res.* 148, 315–333. <https://doi.org/10.1016/j.jvolgeores.2005.05.001>.
- Tassi, F., Montegrossi, G., Capecchiacci, F., Vaselli, O., 2010. Origin and distribution of thiophenes and furans in gas discharges from active volcanoes and geothermal systems. *Int. J. Mol. Sci.* 11, 1434–1457. <https://doi.org/10.3390/ijms11041434>.
- Tassi, F., Capecchiacci, F., Buccianti, A., Vaselli, O., 2012. Sampling and analytical procedures for the determination of VOCs released into air from natural and anthropogenic sources: a comparison between SPME (Soild Phase Micro Extraction) and ST (Solid Trap) methods. *Appl. Geochem.* 27 (1), 115–123. <https://doi.org/10.1016/j.apgeochem.2011.09.023>.
- Tassi, F., Venturi, S., Cabassi, J., Capecchiacci, F., Nisi, B., Vaselli, O., 2015a. Volatile organic compounds (VOCs) in soil gases from Solfatara crater (Campi Flegrei, southern Italy): Geogenic source(s) vs. biogeochemical processes. *Appl. Geochem.* 56, 37–49. <https://doi.org/10.1016/j.apgeochem.2015.02.005>.
- Tassi, F., Venturi, S., Cabassi, J., Vaselli, O., Gelli, I., Cinti, D., Capecchiacci, F., 2015b. Biodegradation of CO₂, CH₄ and volatile organic compounds (VOCs) in soil gas from the Vicano–Cimino hydrothermal system (central Italy). *Org. Geochem.* 86, 81–93. <https://doi.org/10.1016/j.orggeochem.2015.06.004>.
- Templ, M., Filzmoser, P., Reimann, C., 2008. Cluster analysis applied to regional geochemical data: problems and possibilities. *Appl. Geochem.* 23 (8), 2198–2213. <https://doi.org/10.1016/j.apgeochem.2008.03.004>.
- Templ, M., Hron, K., Filzmoser, P., 2011. *robCompositions: an R-package for robust statistical analysis of compositional data*. In: Pawlowsky-Glahn, V., Buccianti, A. (Eds.), *Compositional Data Analysis: Theory and Applications*. John Wiley & Sons Ltd., pp. 341–355.
- Templ, M., Hron, K., Filzmoser, P., Gardlo, A., 2016. Imputation of rounded zeros for high-dimensional compositional data. *Chemom. Intel. Lab. Syst.* 155, 183–190. <https://doi.org/10.1016/j.chemolab.2016.04.011>.
- Venturi, S., 2017. *Volatile Organic Compounds (VOCs) from Volcanic and Hydrothermal Systems: Evidences from Field and Experimental Data*. Doctoral thesis., University of Florence, Italy.
- Venturi, S., Tassi, F., Gould, I.R., Shock, E.L., Hartnett, H.E., Lorange, E.D., Bockisch, C., Fecteau, K.M., Capecchiacci, F., Vaselli, O., 2017. Mineral-assisted production of benzene under hydrothermal conditions: insights from experimental studies on C₆ cyclic hydrocarbons. *J. Volcanol. Geotherm. Res.* 346, 21–27. <https://doi.org/10.1016/j.jvolgeores.2017.05.024>.
- Venturi, S., Tassi, F., Cabassi, J., Vaselli, O., Minardi, I., Neri, S., Caponi, C., Capasso, G., Di Martino, R.M.R., Ricci, A., Capecchiacci, F., Lelli, M., Sciarra, A., Cinti, D., Virgili, G., 2019a. A multi-instrumental geochemical approach to assess the environmental impact of CO₂-rich gas emissions in a densely populated area: the case of Cava dei Selci (Latium, Italy). *Appl. Geochem.* 101, 109–126. <https://doi.org/10.1016/j.apgeochem.2019.01.003>.
- Venturi, S., Tassi, F., Magi, F., Cabassi, J., Ricci, A., Capecchiacci, F., Caponi, C., Nisi, B., Vaselli, O., 2019b. Carbon isotopic signature of interstitial soil gases reveals the potential role of ecosystems in mitigating geogenic greenhouse gas emissions: case studies from hydrothermal systems in Italy. *Sci. Total Environ.* 655, 887–898. <https://doi.org/10.1016/j.scitotenv.2018.11.293>.
- Vogt, C., Kleinstaub, S., Richnow, H.H., 2011. Anaerobic benzene degradation by bacteria. *J. Microbiol. Biotechnol.* 4, 710–724. <https://doi.org/10.1111/j.1751-7915.2011.00260.x>.
- Weelink, S.A.B., van Eekert, M.H.A., Stams, A.J.M., 2010. Degradation of BTEX by anaerobic bacteria: physiology and application. *Rev. Environ. Sci. Biotechnol.* 9, 359–385. <https://doi.org/10.1007/s111>.